JOURNAL OF MATERIALS SCIENCE MATERIALS IN MEDICINE 6 (1995) 8–13

The influence of high sintering temperatures on the mechanical properties of hydroxylapatite

P. VAN LANDUYT, F. LI, J. P. KEUSTERMANS, J. M. STREYDIO, F. DELANNAY
Université catholique de Louvain, Département des sciences des matériaux et des procédés, PCIM, place Sainte Barbe 2, B-1348 Louvain-la Neuve, Belgium

E. MUNTING
Unité de chirurgie orthopédique, Avenue Hippocrate 53, 1200 Bruxelles, Belgium

The kinetics of the thermal decomposition of stoichiometric hydroxylapatite (HA) has been studied up to 1500 °C for the purpose of determining the maximum admissible combinations of temperature and time for sintering HA. The influence of the sintering temperature on shrinkage, density and grain growth is then investigated in the temperature range from 1000 to 1450 °C. Nearly theoretical density was achieved above 1300 °C. A maximum fracture toughness is obtained for the samples sintered at 1300 °C whereas hardness increases up to a sintering temperature of 1400 °C. These results are discussed in terms of the roles of porosity and grain size.

1. Introduction

Hydroxylapatite (HA: $Ca_{10}(PO_4)_6(OH)_2$) is a particularly attractive material for human hard tissue implantation. Indeed, the crystallographic and chemical properties of HA closely resemble those of bone and tooth minerals. Sintered hydroxylapatite thus presents superior compatibility with these tissues. HA is already used in diverse biomedical applications. An important recent development is the use of HA in the form of plasma-sprayed coatings on titanium prostheses. Such coatings are intended to improve the long-term rooting of the prosthesis to the bone. The mechanical properties of these coatings depend on the microstructure and properties of HA, which may be drastically affected by the exposure of the powder to very high temperature during transit in the plasma gun.

Whereas applications of bulk HA ceramics for non-structural implants such as ossicles in the ear pose no particular difficulties, applications for structural implants are hindered by the low strength of sintered HA. Basically, the fracture strength is determined by the maximum flaw size and the fracture toughness. If the sintering process is carried out properly, it can be anticipated that the maximum flaw size will decrease with increasing sintered density, i.e. with increasing sintering time and temperature. However, account should then be taken of the limited stability of HA at high temperature.

The chemical stability of HA during heat treatment at high temperature has been investigated by several authors. 1300 °C is usually considered as the maximum sintering temperature because HA dissociates around this temperature into tricalciumphosphate and tetracalcium phosphate [1, 2]. In a recent paper, Wang and Chaki [3] show that dissociation of HA is very much influenced by the atmosphere, no dissociation being observed at 1300 °C when sintering under moisture.

Literature data on the fracture toughness of HA ceramics remain fairly scarce. Several authors [4–6] have reported fracture toughness data for ceramics sintered at temperatures up to 1300 °C. However, no systematical study of the influence of the sintering temperature on fracture toughness has been published, nor any information about the properties of HA ceramics sintered above 1300 °C.

This work aims at contributing to a more thorough assessment of optimum sintering conditions for achieving the maximum fracture toughness in HA ceramics. First, the thermal stability of stoichiometric HA is studied for the primary purpose of determining the maximum admissible time of exposure at different sintering temperatures. Then, we investigate HA ceramics processed using firing temperatures up to 1450 °C and we discuss the influence of the final density and grain size on the fracture toughness and hardness.

2. Materials and methods

2.1. Processing of the samples

The starting material used in this work is a commercial hydroxylapatite powder (Merck ref. 2196). The calcium and phosphorus contents of the powder were determined by chemical analysis after dissolution in acid (HNO_3 6N). A standard EDTA titration technique was used for measuring the calcium ion concentration. Phosphate concentration was measured using a Beckman ACTA MIV spectrometer. The estimated

0957–4530

relative error in the Ca/PO_4 ratio was 0.65%. Particle size and shape together within the agglomeration state were studied by transmission electron microscopy (TEM). The particles present acicular shapes with an average length of 30 nm and an aspect ratio of about 3 and they are gathered into agglomerates of 0.5 to 1 μm size.

The thermal stability of the powder was assessed by heat treatment in air up to 1500 °C. No control was made of the moisture content of the air in the furnace.

Parallelepipedic bars having final sizes of about 35 × 5 × 6 mm were prepared by sintering. The green bodies were made by isostatic compaction of the powder in a rubber mould under 180 MPa pressure for 2 min. A pre-sintering stage of 2 h at 900 °C in air provided sufficient strength to make possible the dry machining of the bars. The final sintering involved heat treatment in air for 3 h with different temperature dwells between 1000 °C and 1450 °C in such a way as to obtain ceramics with different microstructures and mechanical properties.

2.2. Microstructural characterization

X-ray diffractometry (XRD) was carried out on finely ground samples of the heat treated powders or sintered ceramics using the copper K_α line. Phase identification was made by comparison with the JCPDS files. Lattice parameters d_{hkl} and integrated intensities were calculated by use of the software DIFFRACT 11 from Siemens.

The shrinkage of the sintered samples is defined as $(l - l_0)/l_0$ where l_0 is the length of the green after the pre-sintering stage. The dimensions were measured by use of a micrometer. The apparent density of the samples was determined by the "three weighing" Archimedean method in xylene and the relative density was expressed using 3.16 $g\,cm^{-3}$ for the theoretical density of HA. In each case, the results are the average of measurements performed on five samples.

The grain size distributions were measured by computerized image analysis. For this purpose, the samples were polished with diamond pastes down to 1 μm size. They were then etched during 20 s with a solution of 1 vol % hydrofluoric acid in order to reveal the microstructure. An excellent contrast between the grains and the grain-boundaries was needed on the optical micrographs in order to be able to perform computer image analysis without introducing artifacts. Such a contrast quality could be obtained only for the samples sintered above 1300 °C. Below this temperature, the grain sizes were evaluated on SEM pictures without resorting to image analysis. The image analysis software was based on the method of mathematical morphology introduced by Coster and Chermant [7]. In this method, a cumulative grain size distribution is obtained by carrying out successive "erosions" and "dilatations" on binary images. The actual grain size distribution was obtained by derivation of this cumulative distribution and the mean grain size D was calculated from the distributions.

2.3. Mechanical properties

The toughness K_{Ic} was measured by three-point bending (SENB geometry) using an alumina fixture with a span of 25 mm. Five samples were tested for each sintering temperature. A 1 mm deep notch was cut in the bars using a 0.15 mm thick diamond saw. The straining rate was 0.2 mm/min. The morphology of the fracture surfaces was studied by SEM.

The hardness was determined by Vickers microhardness testing using a load of 5 N. The sample surface was polished with SiC paper to grit 800. The measurements were repeated a number of times sufficient to reach a precision better than 2%. The tests could be carried out only on samples sintered at temperatures above 1200 °C. For lower sintering temperatures, the samples were too porous as to allow accurate measurement of the size of the indentation print.

3. Results

3.1. Composition and thermal stability of the starting HA powder

The theoretical stoichiometric Ca/P ratio in pure HA is 1.67. Commercially available HA powders can be deficient in phosphorus or in calcium ($Ca/P \neq 1.67$) while still yielding an X-ray diffraction spectrum identical to that of pure hydroxylapatite. Alternatively, powders can have the right Ca/P ratio but contain a mixture of tricalcium phosphate, lime, etc. Hence, it was considered important at the beginning of this study to assess the composition of the powders and the nature of the phases that it contained. The Ca/P ratio determined by chemical analysis was 1.68 ± 0.02, hence indicating no departure from stoichiometry. Also, no other phase than HA could be detected on the X-ray diffractograms.

Fig. 1 presents the diffraction peaks within the 2θ range from 27° to 37°. The spectrum at the top (spectrum 1a) is obtained after heat treatment of the

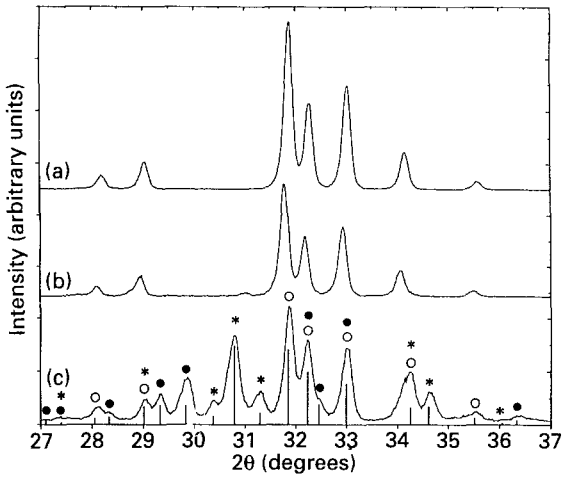

Figure 1 X-ray diffractogram of HA powder after different heat treatment: (a) 2 h at 1300 °C; (b) 8 h at 1300 °C; (c) 8 h at 1500 °C; ○ hydroxyapatite; ● tetracalcium phosphates; * tricalcium phosphate. Bars in the spectrum C represent the position and the relative intensity of the peaks calculated by using the software DIFFRACT 11.

starting powder for 2 h at 1300 °C. The positions of the peaks and their relative intensities correspond very well to the data of the JCPDS files for HA (9-432). For a heating time of 8 h at the same temperature (spectrum 1b), some weak new peaks appear whose intensity is too low to allow identification of the corresponding phases. Fig. 1c presents the spectrum of the powder after heat treatment at 1500 °C for 8 h. The HA appears to have largely decomposed into α-tricalcium phosphate (corresponding to JCPDS 29-359) and tetracalcium phosphate (corresponding to JCPDS 25-1137). The correspondence is rather good for all peaks with 2θ angles ranging from 20° to 60°. This confirms that, when heated at a too high temperature, hydroxylapatite transforms into tricalcium and tetracalcium phosphate according to the scheme [8]:

$$Ca_{10}(PO_4)_6(OH)_2 \rightarrow 2\,\alpha\text{-}Ca_3(PO_4)_2 + Ca_4O(PO_4)_2 + H_2O$$

Fig. 2 shows the variation of the relative intensities of tricalcium phosphate and tetracalcium phosphate as the function of the time of heat treatment at 1500 °C. In this figure, $H_{tric(034)}$ is the relative intensity defined as the ratio of the integral intensity of peak (0 3 4) of tricalcium phosphate to that of peak (2 1 1) of hydroxylapatite. The relative intensity for tetracalcium $H_{tetrac(040)}$ is defined in the same way. The amounts of tricalcium and tetracalcium phosphates remain very small for a duration of heat treatment of 1 h. The concentrations increase then very rapidly between 2 and 4 h of treatment at 1500 °C. Only a slight further increase is observed after 4 h. From these results, it was decided not to exceed 3 h at 1450 °C for sintering the ceramics.

3.2. Microstructure of the sintered samples

Fig. 3 shows the X-ray diffractogram of a sample sintered for 3 h at 1450 °C (i.e. under the most severe conditions used in this study). As anticipated from the preliminary study, no decomposition of HA is observed. It can thus be considered that the mechanical properties will not be affected by the presence of secondary phases.

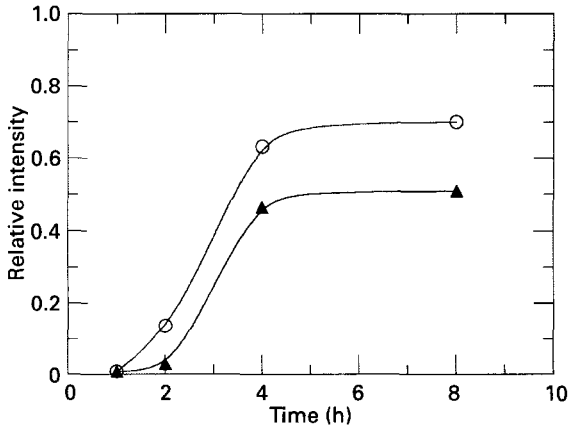

Figure 2 Variation of the relative intensities of tricalcium and tetracalcium phosphate peaks as a function of the time at 1500 °C. $H_{tric(034)}$ (○) and $H_{tetra(040)}$ (▲) are the ratios of the integral intensity of, respectively, peak (0 3 4) of tricalcium phosphate or peak (0 4 0) of tetracalcium phosphate to the intensity of peak (2 1 1) of hydroxylapatite.

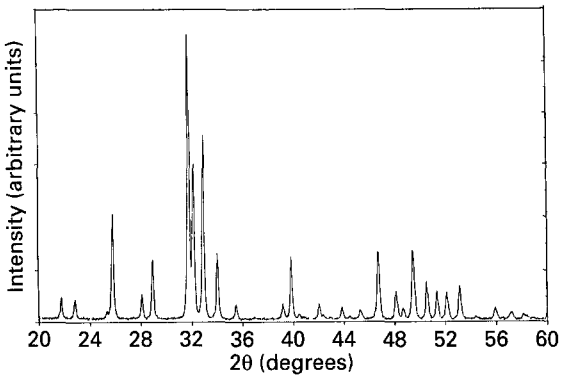

Figure 3 X-ray diffractogram of a sample sintered for 3 h at 1450 °C.

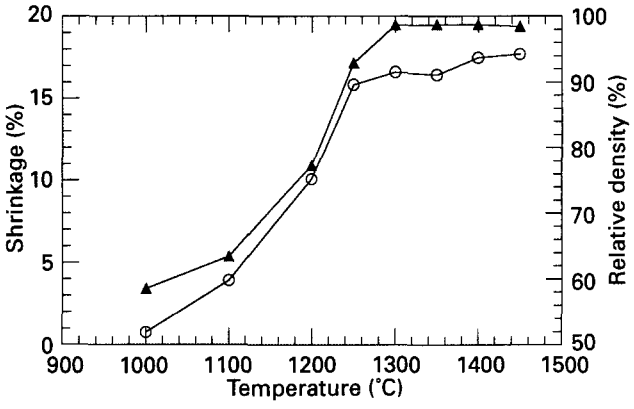

Figure 4 Variation of shrinkage (○) and relative density (▲) of the ceramics as a function of the sintering temperature.

Fig. 4 shows the variations of the relative density and shrinkage as a function of the sintering temperature. The relative density measured by the Archimedean method increases from 57% after presintering at 900 °C to nearly 99% after sintering at 1450 °C. Such a density is high in comparison to the values usually reported in the literature for HA ceramics sintered up to 1300 °C [1, 3, 4, 6]. The linear shrinkage increases from 0.77% at 1000 °C to 17.7% at 1450 °C. It was verified that the shrinkage during sintering was homothetic, owing to the isostatic pressing of the green sample. The two curves in Fig. 4 present the same sigmoïdal shape with an inflexion point around 1200 °C. Indeed, it may be calculated that the shrinkage values agree very well with the density values. For example $(100\%-17.7\%)^3 = 56\%$: both density and shrinkage measurements thus indicate that nearly full density was achieved after sintering at high temperature.

Fig. 5 presents the grain size distributions obtained by image analysis for the samples sintered above 1300 °C. For a sintering temperature of 1300 °C, the distribution presents a fairly narrow unimodal curve whereas a widening of the distribution appears for higher sintering temperatures. This widening is particularly important at 1450 °C. As illustrated in the micrograph in Fig. 6, this phenomenon is related to

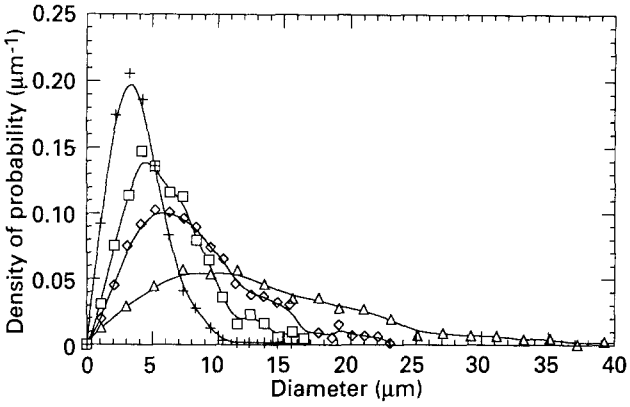

Figure 5 Distribution of the grain sizes in ceramics sintered at 1300 °C (+); 1350 °C (—□—); 1400 °C (—◇—); 1450 °C (—△—).

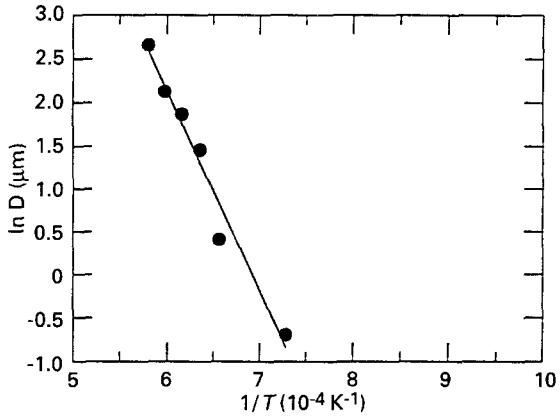

Figure 7 Arrhénius plot of the variation of the mean grain size D as a function of the temperature.

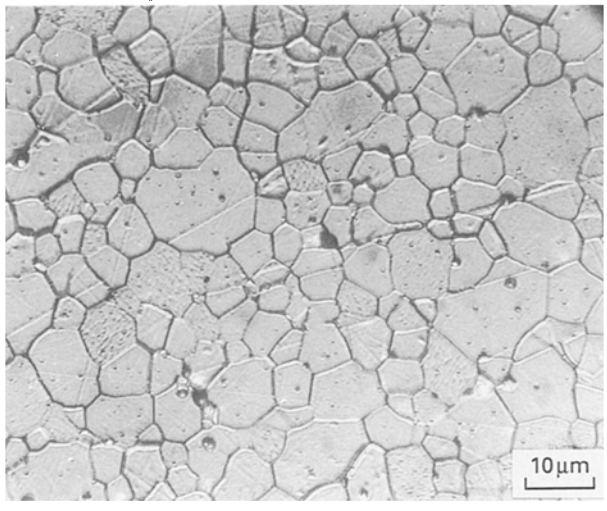

Figure 6 Exaggerated grain growth in a sample sintered for 3 h at 1450 °C.

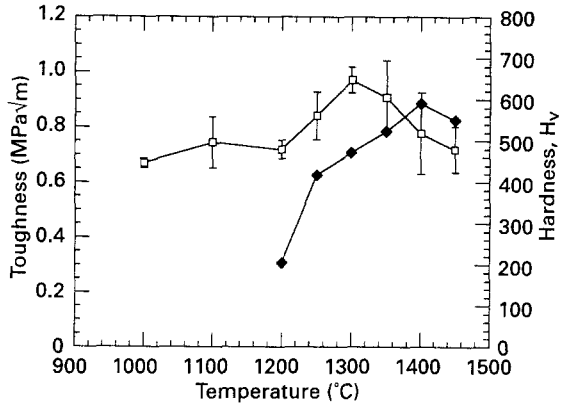

Figure 8 Variation of fracture toughness (□) and Vickers hardness (◆) as a function of the sintering temperature.

the occurrence of exaggerated grain growth at this temperature. Fig. 7 presents an Arrhénius plot of the variation of the mean grain size D as a function of the sintering temperature. D increases steadily from 4 μm to 14 μm when the sintering temperature increases from 1300 °C to 1450 °C.

3.3. Mechanical properties

The slope of load–displacement curves during toughness testing exhibited an inflexion point at the onset of cracking, indicating that linear elastic fracture mechanics applies. The variation of K_{Ic} as a function of the sintering temperature is presented in Fig. 8. The error bars represent the standard deviations on five tests. K_{Ic} increases first from 0.67 MPa$\sqrt{m}$ for the samples sintered at 1000 °C to a maximum of 0.97 MPa$\sqrt{m}$ for the samples sintered at 1300 °C. It appears then to decrease slightly to about 0.72 MPa $\sqrt{m}$ for the samples sintered at 1450 °C. The SEM micrograph of the fracture surfaces presented in Fig. 9 indicates that the fracture mode is fully transgranular.

Fig. 8 shows also the variation of the Vickers hardness as a function of the sintering temperature. In

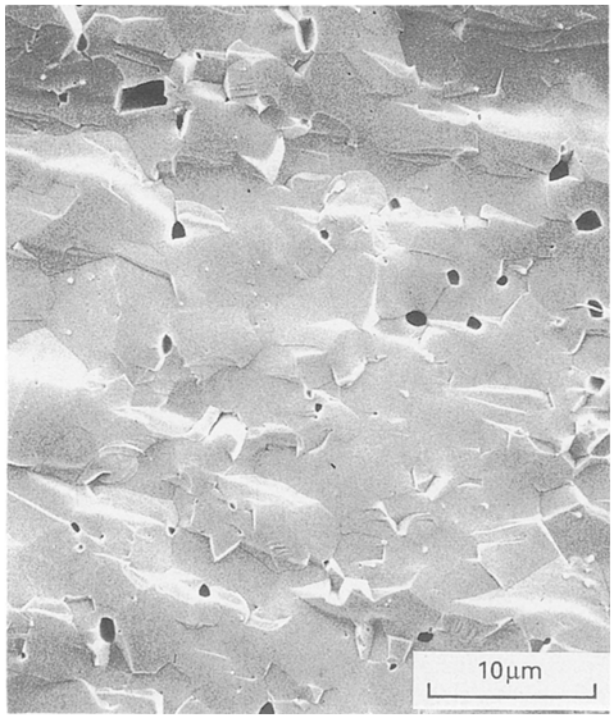

Figure 9 SEM micrograph of the fracture surface of a sample sintered for 3 h at 1350 °C.

contrast to K_{Ic}, hardness increases steadily up to 1400 °C. The diagonal size of the Vickers prints remains larger than the mean grain size even for the samples having the largest grain sizes. For example, for the sample sintered at 1450 °C, the mean diagonal size of the prints is 41 μm whereas the mean grain size is 14 μm. (However, as shown on the size distribution in Fig. 5, a small proportion of the grains can reach a diameter larger than 40 μm.)

4. Discussion

4.1. Thermal stability of HA

It has been reported in the literature that hydroxylapatite starts decomposing around 1200 °C when heat-treated in O_2 for 6 h [1] or in dry air for 4 h [3]. In the present study, stoichiometric hydroxylapatite sintered in air is shown to decompose only slightly when heat-treated at 1300 °C for 8 h. The incubation time before the beginning of decomposition is more than 3 h for treatment at 1450 °C (Fig. 3), but only about 1 h at 1500 °C (Fig. 2). The influence of the moisture content of the atmosphere on the stability of HA at high temperature has been demonstrated by Wang and Chaki [3]. As no particular control of the air atmosphere in the sintering furnaces was made in the present work, the results indicate that the minimum moisture content for allowing such a stabilization is fairly low.

The incubation time observed in Fig. 2 for heat treatment at 1500 °C is typical of a reaction governed by nucleation and growth mechanisms. One can also observe that the dissociation appears to level off after about 4 h, with a significant amount of HA remaining stable for longer sintering times. This slowing down of the decomposition rate may be related to the grain growth of non-transformed HA which was shown to occur simultaneously during heat treatment. The stabilizing effect of grain growth suggests that the dissociation of HA nucleates primarily on crystal defects and grain boundaries. It may be anticipated that a similar incubation phenomenon will be observed at all temperatures, with a decrease of the incubation time when the heat treatment temperature increases. This can explain why pure HA can be maintained in coatings processed by plasma-spraying if the duration of exposure of the powder at high temperature in the plasma torch is sufficiently short. Studies of the kinetics of the decomposition of HA at higher temperatures would be needed in order to get an estimation of the maximum allowable time of transit of the powder in the torch.

4.2. Densification and grain growth

Fig. 4 shows that, in agreement with the literature, little densification occurs during sintering at 1000 °C and 1100 °C. Below this temperature, sintering is limited to the first stage of sintering, which corresponds to the mere formation of solid bridges between the grains. On another hand, the densities obtained after sintering at or above 1300 °C are high in comparison with the densities reported in the literature for HA sintered up to 1300 °C (whatever the nature of the atmosphere). In addition to the effect of the higher temperatures used in the present study, this result is due also to the very fine grain size of the starting powder. According to Wang and Chaki [3], as long as no dissociation occurs, sinterability is also favoured by some dehydroxylation of HA, a phenomenon which could have occurred in the present study owing to the limited moisture content of the sintering atmosphere. Only limited further progress of the densification is observed above 1300 °C. As observed in Figs 6 and 9, this is due to the separation of the residual pores from the grain boundaries as a consequence of the increase of the grain sizes (Fig. 7).

The average grain sizes measured after sintering at high temperature are fairly high for sintered HA. The activation energy calculated from the Arrhénius plot of Fig. 7 amounts to 47 kcal/mol. This value, which should correspond to the activation energy for diffusion in HA, is in agreement with the values of 56 and 57 kcal/mol reported by Jarcho *et al.* [9] and Kijima and Tsutsumi [10], respectively, for the temperature range up to 1300 °C. It deviates significantly from the value of 34 kcal/mol measured by De With *et al.* [4].

4.3. Mechanical properties

The variation of the fracture toughness as a function of the sintering temperature is due to the combined influences of density and grain size.

Let us consider first the temperature range between 1000 °C and 1300 °C within which the density increases from 60% up to more than 98% while the grain size remains below a few micrometers. One observes a 40% increase of K_{Ic} from 0.67 to 0.97 $MPa\sqrt{m}$, whereas hardness increases by more than 200% in the same temperature range. The increase of K_{Ic} appears thus fairly limited. Indeed, it has been reported that the fracture toughness K_{Ic} of sintered materials decreases only slightly with increasing porosity [11–13]. Accounting for the drastic decrease of the elastic modulus E with increasing porosity, this means that the critical energy release rate may even increase with increasing porosity [12]. This effect appears to be due to crack tip shielding as a result of the meandering of the crack in the porosity.

No further density change is observed in the temperature range from 1300 °C to 1450 °C. Meanwhile, the grains grow from 4 to 14 μm. This grain growth appears to cause a 25% decrease of K_{Ic} from 0.97 to 0.72 $MPa\sqrt{m}$. A decrease of K_{Ic} with increasing grain size is usually observed in ceramics when the fracture mechanism is transgranular because the major contribution to cracking resistance is then related to the crossing of the grain boundaries [14]. The maximum value of fracture toughness obtained at 1300 °C is in agreement with the values reported in the literature [4–6] for samples sintered up to 1300 °C, although these samples presented usually a lower relative density than the values achieved in the present work. This indicates that optimization of fracture toughness requires that full density be reached while keeping a minimum of grain size. Short duration pressure

sintering at high temperature might be beneficial if a sufficient moisture content can be maintained in the hot press.

The increase of hardness by more than 200% when the sintering temperature increases from 1000 °C to 1300 °C is obviously due to the decrease of the porosity. This observation is quite classical for sintered materials [13]. In contrast, the further increase of hardness between 1300 to 1400 °C cannot be ascribed to densification. It can be interpreted as due to the combined effect of flaw size and fracture toughness. If the ceramic is fully dense, the fracture strength should decrease when the fracture toughness decreases and when the critical flaw size increases. No fracture strength measurements have been carried out in this work. However, according to Rice [15], the compressive strength of a ceramic scales with its hardness. The increase of the hardness in spite of the decrease of fracture toughness may thus be justified if the critical flaw size scales with the sizes of the residual pores, which keep decreasing with the increase of the density when the sintering temperature increased (Fig. 4). Rice [15] suggests that the compressive strength of a ceramic can be estimated by merely dividing the Vickers hardness value by a factor of 3. According to this rule of thumb, the strength of samples processed in this work would peak at around 200 MPa for sintering at 1400 °C.

5. Conclusions

This work demonstrates that pure HA ceramics presenting nearly full density can be obtained by sintering above 1300 °C. The grain size increases steadily beyond 1300 °C, whereas exaggerated grain growth is observed at 1450 °C. Under the air atmosphere used in this work, only a slight dissociation was observed after 8 h at 1300 °C, whereas pure HA was kept in the ceramic after a sintering time of 3 h at 1450 °C. The dissociation of HA occurs by a nucleation and growth mechanism, involving an incubation period whose duration decreases with increasing temperature.

For the dense samples, the highest fracture toughness is obtained with the smallest grain sizes, i.e. after sintering at 1300 °C. However, due to the decrease of the maximum flaw size with decreasing pore size, the hardness (i.e. also the compressive strength) keeps increasing up to an optimum value for a sintering temperature of 1400 °C.

References

1. J. G J. PEELEN, B V REJDA and K DE GROOT, *Ceramurgia Int.* **4** (1978) 71.
2. K. DE GROOT, *Biomaterials* **1** (1980) 47
3. PAUCHIU E WANG and T K. CHAKI, *J. Mater. Sci. Mater. Med.* **4** (1993) 150.
4. G. DE WITH, J A VAN DIJK, H. N HATTU and K. PRIJS, *J Mater Sci.* **16** (1981) 1592.
5. M B. THOMAS and R H DOREMUS, *Ceram. Bull.* **60** (1981) 258.
6. M AKAO, N MIURA and H. AOKI, *Yogyo Kyokai Shi* **92** (1984) 672.
7. M COSTER and J. L CHERMANT, in "Précis d'analyse d'images" (CNRS, Paris, 1985).
8. J R VAN WAZER, in "Phosphorus and its compounds, Vol. I: Chemistry" (Interscience Publishers, New York, 1958) p. 527.
9. M. JARCHO, C H BOLEN, M. B THOMAS, J BOBICK, J F KAY and R H. DOREMUS, *J. Mater. Sci.* **11** (1976) 2027.
10. T KIJIMA and M. TSUTSUMI, *J. Amer. Ceram Soc.* **62** (1979) 455.
11. R HAYNES, in "Reviews of the deformation behaviour of materials", Vol. 3, edited by P. Feltman (Freund, Tel Aviv, Israel, 1981) pp. 9–101.
12. L CORONEL, J. P. JERNOT and F. OSTERSTOCK, *J. Mater Sci.* **25** (1990) 4866.
13. R MORELL, in "Handbook of properties of technical and engineering ceramics: part 1: an introduction for the engineer and designer" (Her Majesty's Stationary Office, 1985)
14. S W FREIMAN, *Ceram. Bull.* **67** (1988) 392.
15. R. W RICE, in "Materials science research, Vol. 5: The compressive strength of technical and engineering ceramics" (Plenum, New York, 1971) p 195.

Received 27 October 1992
and accepted 16 January 1994